Applied Catalysis B: Environmental 142–143 (2013) 337–343

Contents lists available at SciVerse ScienceDirect

Applied Catalysis B: Environmental

journal homepage: www.elsevier.com/locate/apcatb

Experimental and modeling study of a dual-layer (SCR + PGM) NH_3 slip monolith catalyst (ASC) for automotive SCR after treatment systems. Part 2. Validation of PGM kinetics and modeling of the dual-layer ASC monolith

Massimo Colombo[a], Isabella Nova[a], Enrico Tronconi[a,*], Volker Schmeißer[b], Brigitte Bandl-Konrad[b], Lisa Rahel Zimmermann[c]

[a] Dipartimento di Energia, Laboratorio di Catalisi e Processi Catalitici, Politecnico di Milano, Piazza Leonardo da Vinci 32, I-20133 Milano, Italy
[b] Daimler AG, 019-G206 RD/RPE, 70546 Stuttgart, Germany
[c] Daimler AG, 019-D121 TP/PME, 70546 Stuttgart, Germany

ARTICLE INFO

Article history:
Received 7 February 2013
Received in revised form 10 May 2013
Accepted 16 May 2013
Available online 23 May 2013

Keywords:
Ammonia slip catalyst
Urea SCR
Dual layer monolith
Ammonia oxidation
Diesel exhaust after treatment

ABSTRACT

We present herein the final part in the development and validation of a chemically and physically consistent mathematical model of a commercial dual-layer (SCR + PGM) monolithic NH_3 slip converter (ASC). Specifically, in this conclusive Part 2 of the project we first validate the global kinetic model for the PGM catalyst component, previously developed in Part 1 over the precursor powders, against data collected over a single-layer coated monolith. Then, we incorporate validated kinetics for the two individual SCR and PGM components into a dual-layer ASC monolith catalyst model and proceed to a systematic validation against experimental catalytic activity data collected over core samples of the dual-layer ASC system. A DOE approach is also adopted in order to secure a uniform coverage of the operating field.

A positive interaction of the PGM and SCR catalytic chemistries is emphasized by the data collected over the dual-layer SCR + PGM monolith catalyst, leading to largely enhanced N_2 selectivities as compared to a single-layer PGM-only washcoat. We show that such a beneficial interaction between the PGM and SCR chemistries occurs via diffusion/reaction of NH_3 and NO_x in the SCR catalyst layer. Results prove that the dual-layer ASC model can simulate realistically the actual NH_3 slip catalyst configuration over a wide range of representative conditions.

1. Introduction

Selective catalytic reduction by NH_3 (NH_3-SCR) has become an established process for the after treatment of NO_x coming from passenger cars as well as from heavy duty vehicles. In order to prevent any undesired emission of the reducing agent (i.e. NH_3) into the environment, a so-called NH_3 slip catalyst (ASC) can be placed as a small monolith slice after the SCR to oxidize NH_3 having left the SCR brick [1]. It has been recently proposed that the combination of a precious metal containing washcoat with a SCR washcoat in a dual-layer architecture enables minimal NH_3 breakthrough at increased NO_x conversion of the after treatment system [2–5]. The present paper is part of a work aimed at the development of a chemically consistent mathematical model of such dual-layer ASC converters. This work involved first the activity study and kinetic modeling of the SCR component of the ASC system [6], namely a state-of-the-art Fe-zeolite catalyst. Then, in a second stage, the PGM component of the ASC system was studied under typical automotive conditions and a consistent kinetic model was developed. In addition, the potential interactions of PGM and SCR catalytic chemistries were also studied by means of two different reactor configurations, involving either the sequential use the two catalysts or their intimate mixing [7]. The third stage of the work involved the integration of the developed SCR/PGM kinetics in a specifically developed mathematical model of dual-layer monolith catalysts [8]. The last stage of the work, which represents the specific object of the present contribution, has involved the final validation of the developed mathematical model against experimental data collected over the single layered PGM monolith as well as over the full dual-layer ASC monolith catalyst. The validation of the SCR kinetics was instead reported in [6].

* Corresponding author. Tel.: +39 02 2399 3264; fax: +39 02 2399 3318.
E-mail address: enrico.tronconi@polimi.it (E. Tronconi).

0926-3373/$ – see front matter © 2013 Elsevier B.V. All rights reserved.
http://dx.doi.org/10.1016/j.apcatb.2013.05.032

2. Methods

2.1. Experimental

The dual-layer ASC system herein studied was composed of commercial state-of-the-art PGM and SCR catalysts: the PGM catalyst was a Pt/Al_2O_3 based system, while a Fe-zeolite was used as the NH_3-SCR catalyst. Two catalyst samples, supplied in the form of washcoated cordierite monoliths (400 CPSI, wall thickness = 5 mils), were tested in the present work. One was coated with the PGM phase only, whereas the other sample was coated with the SCR catalyst layer on top of the PGM layer. With the latter monolith, which represents the real configuration of the investigated dual-layer ASC system, additional validation experiments according to a DOE-plan have been performed. All experiments on the monolith samples have been carried out in a synthetic gas rig with a quartz glasstubular reactor at Daimler, Stuttgart. In this rig the temperature of the sample is detected 2 mm in front of the monolith inlet and 5 mm behind the monolith outlet. The instrumental set-up for gas phase analysis of NH_3 (MIPANQA100, Prometh), NO_x (CLD700 El ht, ecophysics) and N_2O (Binos, Fisher-Rosemount) was used for detection of steady-state product species behind the monolith. The samples were pre-conditioned for 5 h at 600 °C with a mixture of 8% (v/v) H_2O and N_2. Most of the experimental runs consisted of isothermal steady-state experiments in the 150–550 °C temperature range. A constant flow rate and feed gas composition was fed to the reactor at a constant temperature until steady state conditions were reached at reactor outlet. Then, the temperature was changed to a new set point and a new steady state condition was reached. A few experiments were also performed applying a slow temperature ramp (2 °C/min) from 150 to 550 °C while keeping constant gas flow rate and composition. Thanks to the low heating rate, these experiments were found to be essentially equivalent to steady state runs over the whole 150–550 °C temperature range.

In order to expand the ASC DoE-measurements within a wide range of space velocities two samples were used with a diameter of 22.5 mm and a length of 15.1 and 60.4 mm, respectively. The homogeneity of both samples was checked by comparison of NH_3 adsorption at 200 °C and NH_3 oxidation performance at 400 °C, under the same space velocity conditions. The DOE plan varied the main operating parameters such as temperature, space velocity, NH_3/NO_x and NO_2/NO_x feed ratios. The detailed description of the DOE operation points is reported in Section 3.3.

2.2. Kinetic and reactor models

Kinetic schemes developed in Refs. [6,7] were used to model the catalytic activity of the SCR and of the PGM component of the studied ASC system, respectively. The validation of the SCR kinetics, originally developed over the catalyst in a powdered form, was presented in Ref. [6]: the kinetics were implemented in a heterogeneous dynamic 1D + 1D model of a single monolith channel, accounting also for external (gas–solid) and internal (intra-porous) mass transfer resistances. Model simulations were then systematically compared with experimental data collected over core monolith samples coated with the same Fe-zeolite SCR catalyst.

A similar approach is used in this paper to validate the PGM kinetics developed in [7] over a powdered catalyst: experimental data collected over a PGM-coated monolith are systematically compared in the following with predictive model simulations. However, a different reactor model was used in this case. Indeed, a simulation analysis of PGM coated monolith catalysts [8] has pointed out that that the extremely high reaction rates over this catalytic system result in a fully diffusion-controlled regime above 250 °C. For this reason, we assumed that in the case of washcoated monolith samples only the PGM washcoat surface was effectively active, and we treated accordingly the PGM layer as a surface. The kinetics developed over the powdered PGM catalyst was thus referred to the catalyst geometrical surface area and directly included in the PGM monolith model. Notably, in the case of the tested PGM monolith the surface reaction approximation was however valid also at temperatures below 250 °C, where the system operates in a chemical regime [8]. Indeed, as pointed out in Section 2.1 of Ref. [7], the PGM kinetics was studied on a catalyst powder sieved to 140–200 mesh. This corresponds to an average particle diameter of 90 μm which, assuming a spherical geometry for the catalyst powder, results in a volume to surface ratio of 15 μm. The tested PGM monolith sample was characterized by a washcoat thickness of about 15 μm: since the washcoat thickness corresponds to the catalyst volume to surface ratio in the case of a washcoated monolith, the surface reaction approximation was valid in our case also at temperatures below 250 °C.

This approach for the PGM component was adopted also for the development of the mathematical model of the dual-layer ASC catalysts, presented by some of us in [8]. Such a model, named LSM (Layer + Surface Model), was based on the mathematical model of SCR monolithic converters described by Chatterjee et al. [9–11]: the presence of the PGM layer, regarded as a surface, was directly included in the mentioned SCR converter model by simply modifying the inner boundary condition for the diffusion-reaction equations in the SCR layer, i.e. the one at the interface between the SCR and the PGM phase. It is worth noting that the same dual-layer LSM model reduces to the PGM monolith model when the SCR layer thickness approaches zero.

3. Results and discussion

3.1. Validation of PGM kinetics

In analogy to the procedure followed in Ref. [6] for the SCR component of the dual-layer ASC, the PGM kinetics, developed over a powdered catalyst, were validated against experimental data collected over a core monolith sample coated only with the PGM component of the ASC.

Experimental data were collected according both to steady state and transient test protocols. A wide range of operating conditions was covered in terms of temperature (150–550 °C) and feed compositions (NO_x/NH_3 = 0–1 with NO_2/NO_x between 0 and 1).

Figs. 1–3 show the comparison between experimental results (dashed lines and dots) and predictive model simulations (solid lines) in terms of NH_3 conversion and products yields measured at the monolith outlet. The results are plotted as a function of the monolith temperature. As N_2 was not measured in this work, the N_2 yield shown here has been calculated by subtracting the sum of yields of all other species from 1.

In Fig. 1, an NH_3 oxidation test is displayed: the monolith temperature was linearly increased from 150 °C up to 550 °C at a constant rate of 20 K/min while continuously feeding to the reactor a N_2 stream containing 500 ppm of NH_3 and 8% (v/v) of H_2O, O_2 and CO_2 for a volumetric space velocity of 60,000 h^{-1}.

Focusing on dashed lines, representing experimental data, it can be noticed that NH_3 conversion started above 160–175 °C and rapidly increased up to 80% already at 200 °C, before approaching 100% at 350 °C. NH_3 conversion is associated with production of N_2, N_2O and NO_x, the main product being a function of the monolith temperature: the N_2 maximum yield is approached around 200 °C, followed by that of N_2O centered around 275 °C, while NO_x become the main oxidation product above 350 °C, with a yield close to 100% at the highest investigated temperature [4,7].

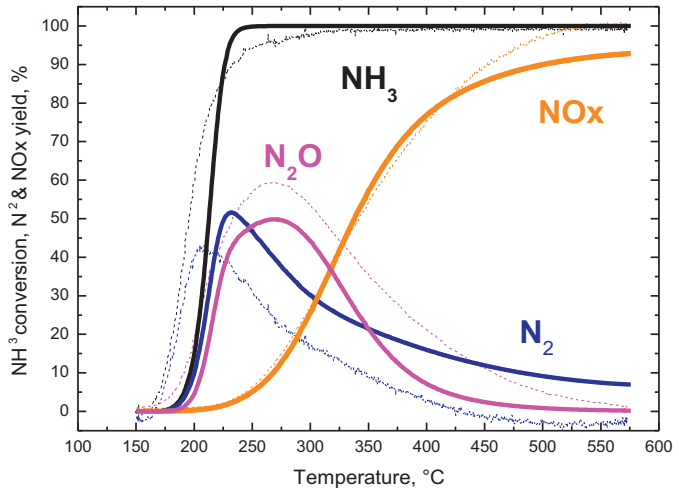

Fig. 1. NH_3 oxidation on PGM monolith. NH_3 = 500 ppm; H_2O = 8% (v/v); O_2 = 8% (v/v); CO_2 = 8% (v/v), GHSV = 60,000 h^{-1} (N_2 amount calculated from N-balance). Thin lines: experimental results; thick lines: model simulations.

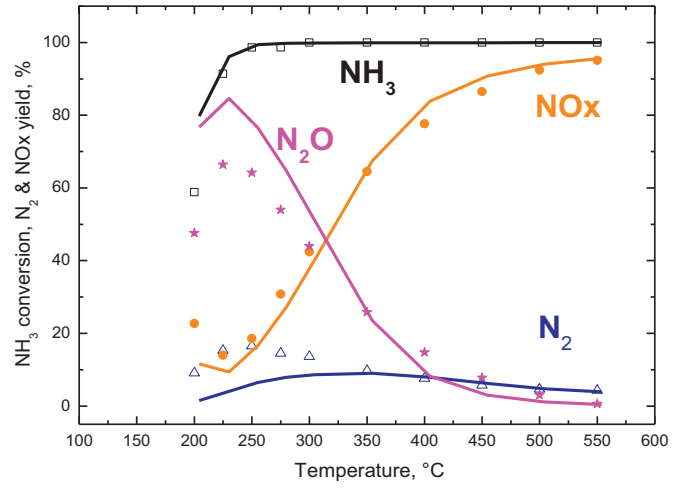

Fig. 2. NH_3/NO_x reacting system on PGM monolith. NH_3 = 500 ppm; NO_x = 500 ppm; NO_2/NO_x = 0; H_2O = 8% (v/v); O_2 = 8% (v/v); CO_2 = 8% (v/v), GHSV = 100,000 h^{-1}(N_2 amount calculated from N-balance). Symbols: experimental results; lines: model simulations.

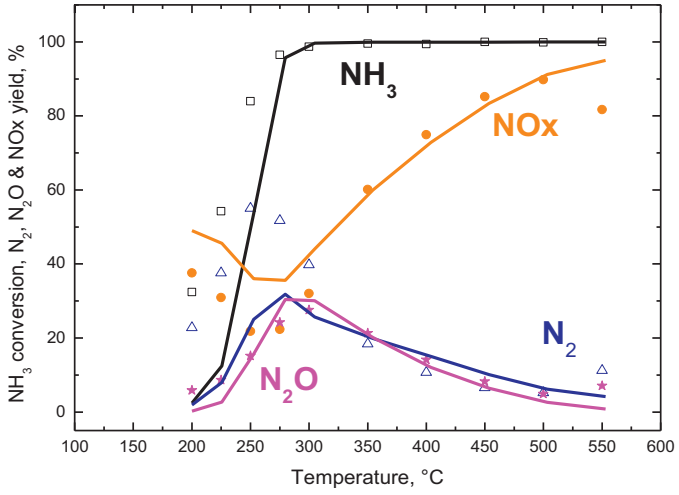

Fig. 3. NH_3/NO_x reacting system on PGM monolith. NH_3 = 500 ppm; NO_x = 500 ppm; NO_2/NO_x = 1; H_2O = 8% (v/v); O_2 = 8% (v/v); CO_2 = 8% (v/v), GHSV = 100,000 h^{-1}(N_2 amount calculated from N-balance). Symbols: experimental results; lines: model simulations.

The same qualitative trends are also shown by model simulations (Fig. 1, thick solid lines). From the quantitative point of view the model slightly overestimated the light off temperature of NH_3 conversion, with subsequent underestimation of the N_2 yield in the 150–200 °C *T*-range. Above 250 °C the model overestimates the N_2 yield at the expense of the N_2O yield, while an almost perfect match between experiments and simulations is observed for the NO_x yield, at least up to 450 °C. Above this temperature the model slightly underestimates the NO_x production. Overall, the agreement between experiments and predictive model simulations was considered to be satisfactory.

The effect of NO_x addition to the feed stream was then investigated as a function of temperature in the range 200–550 °C and NO_2/NO_x ratio (from 0 to 1) by means of steady state experiments where a stream containing 500 ppm of NH_3 and NO_x were continuously fed to the reactor with 8% (v/v) of H_2O, O_2 and CO_2 in N_2, with a space velocity of 100,000 h^{-1}.

Fig. 2 shows experimental (dots) and modeling (solid lines) results obtained with NO as the only NO_x source at monolith inlet (NO_2/NO_x = 0): looking at the experimental results, a high NH_3 conversion (about 60%) was observed already at 200 °C, with complete consumption of the same species above 250 °C. NO consumption was also evident below 300 °C, where the NO_x yield was below 50% (yield corresponding to the amount of NO fed to the reactor). On the opposite at higher temperatures the same species became the main product, with yields above 90%. Over the whole *T*-range the N_2 yield was low, with a maximum of about 20% at 250 °C, while below 300 °C the main reaction product was N_2O with yields up to almost 70%.

The presence of NO_2 in the feed mixture resulted in a change of both activity and selectivity, as shown in Fig. 3 where the symbols represent the experimental data collected feeding 500 ppm of NH_3 and NO_x each with 8% (v/v) of H_2O, O_2 and CO_2 in N_2, with NO_2/NO_x = 1 (see supplementary material for the case of NO_2/NO_x = 0.25 (Figure A), 0.5 (Figure B) and 0.75 (Figure C)).

As an example, the NH_3 conversion showed a maximum of about 85% at 200 °C for a NO_2/NO_x ratio of 0.25 (Figure A in supplementary material), and then progressively decreased at increasing NO_2/NO_x ratio to about 35% in the case of NO_2 as the only NO_x species (Fig. 3). Also the conversion of NO_x decreased below 300 °C with increasing NO_2 feed content, while at high temperatures yields around 100% were always obtained, independent of the amount of NO_2 in the feed stream. The addition of NO_2 as a NO_x source resulted in a positive impact on products selectivity below 350 °C, favoring the formation of desired N_2 at the expenses of undesired N_2O.

Experimental data were then compared with predictive simulations (solid lines in Figs. 2–3). A slight but systematic underestimation of NH_3 and NO_x conversions was observed below 250 °C, with the exception of the test performed in the absence of NO_2 in the feed stream, where the opposite deviation was observed (Fig. 2). A good agreement between experimental data and model simulations was recorded in terms of N_2, N_2O and NO_x yields above 250 °C, while a general underestimation of N_2 production was observed below that temperature. Such a deviation is however related to the underestimation of the NH_3 conversion in the same temperature region (see supplementary material for the case of NO_2/NO_x = 0.25 (Figure A), 0.5 (Figure B) and 0.75 (Figure C)).

Summarizing the validation results over the PGM monolith catalyst, a satisfactory agreement between predictive model simulations and experimental data was observed above 300 °C for all the investigated feed compositions. On the opposite, at lower temperatures slight deviations were noted mainly in terms of NH_3 conversion, resulting however in acceptable errors.

3.2. Performance comparison of PGM and dual-layer monolith catalysts

As already discussed in Section 1, the purpose of a dual-layer SCR + PGM architecture in NH_3 slip monolith catalysts is to increase the selectivity of the ammonia oxidation process toward N_2. However, as a drawback, the addition of the SCR component on top of the PGM coating can result in a decrease of the overall oxidation activity, since the SCR layer acts as a diffusion barrier for NH_3 approaching the PGM surface [1]. In order to understand the impact of the SCR catalyst addition on products selectivity and to assess the importance of diffusional limitations under typical operative conditions, the catalytic performances of the PGM only coated monolith were directly compared with those of the dual-layer system. Specifically, a systematic set of steady state catalytic tests was carried out in the 200–550 °C *T*-window feeding a stream containing 500 ppm of NH_3 and NO_x with 8% (v/v) of H_2O, O_2 and CO_2 in N_2, with a space velocity of 100,000 h^{-1}, for feed NO_2/NO_x ratios ranging from 0 to 1. The corresponding results in terms of NH_3 conversion and products yields are shown in Figs. 4 and 5 (thick lines), where they are compared with those collected over the PGM-only monolith (thin lines in Figs. 4 and 5 and symbols in Figs. 2 and 3). The same results for the cases of NO_2/NO_x = 0.25, 0.5 and 0.75 are provided as supplementary material (Figures D, E and F respectively).

Fig. 4 displays the comparison for NO_2/NO_x = 0, i.e. only NO and NH_3 were fed to the reactor. The NH_3 conversion activity measured over the dual-layer system (thick lines) was comparable to that observed over the PGM only monolith (thin lines), as evident from inspection of Fig. 4A: high NH_3 conversion (about 60%) was recorded already at 200 °C, while complete consumption of the reactant was measured over both systems above 250 °C. On the opposite, a dramatic effect of the SCR layer addition on top of the PGM one was observed in terms of products selectivity (Fig. 4B–D) for the same reacting system. In the whole *T*-range the N_2 yield recorded over the dual-layer monolith (Fig. 4B) was significantly greater compared to that observed over the PGM catalyst, with differences as high as 50%. The increased N_2 yield resulted in the decrease of both NO_x and N_2O yields. In the case of NO_x a maximum yield of about 45% was reached at 550 °C, against a value close to 100% in the case of the PGM only monolith. The N_2O yield was constantly lower in the case of the dual-layer system, with the maximum value reduced from 70% down to 45%.

When both NO and NO_2 were simultaneously present at the dual-layer NH_3 slip catalyst inlet (Figures D and F in supplementary material), a strong enhancement of both NH_3 conversion and N_2 yield was recorded over the whole 200–550 °C *T*-range. More specifically, the enhancement of NH_3 conversion was evident in the low-T region, while at temperatures higher than 300 °C the comparison was limited by the complete conversion observed over both catalytic systems. The decrease of undesired products yields was extremely evident in terms of both NO_x and N_2O, with the yield of the latter species close to zero for NO_2/NO_x equal to 0.5 and 0.75 (Figures E–F in supplementary material).

When NO_2 was the only NO_x source at catalyst inlet (Fig. 5), the presence of the SCR layer on top of the PGM one resulted in a slight decrease of NH_3 conversion between 225 and 300 °C (Fig. 5A), while the positive effect in terms of N_2 selectivity, already discussed for other reacting systems, was confirmed over the whole 200–550 °C *T*-range (Fig. 5B). Increases of the N_2 yield as high as 70% were recorded in comparison with the PGM only configuration, associated with corresponding reductions of both NO_x (Fig. 5C) and N_2O (Fig. 5D) yields, with the higher absolute improvements observed for the former species.

Summarizing the comparison of catalytic performances of PGM and dual-layer SCR + PGM monoliths, the addition of the SCR layer on top of the PGM one resulted in a clear improvement of

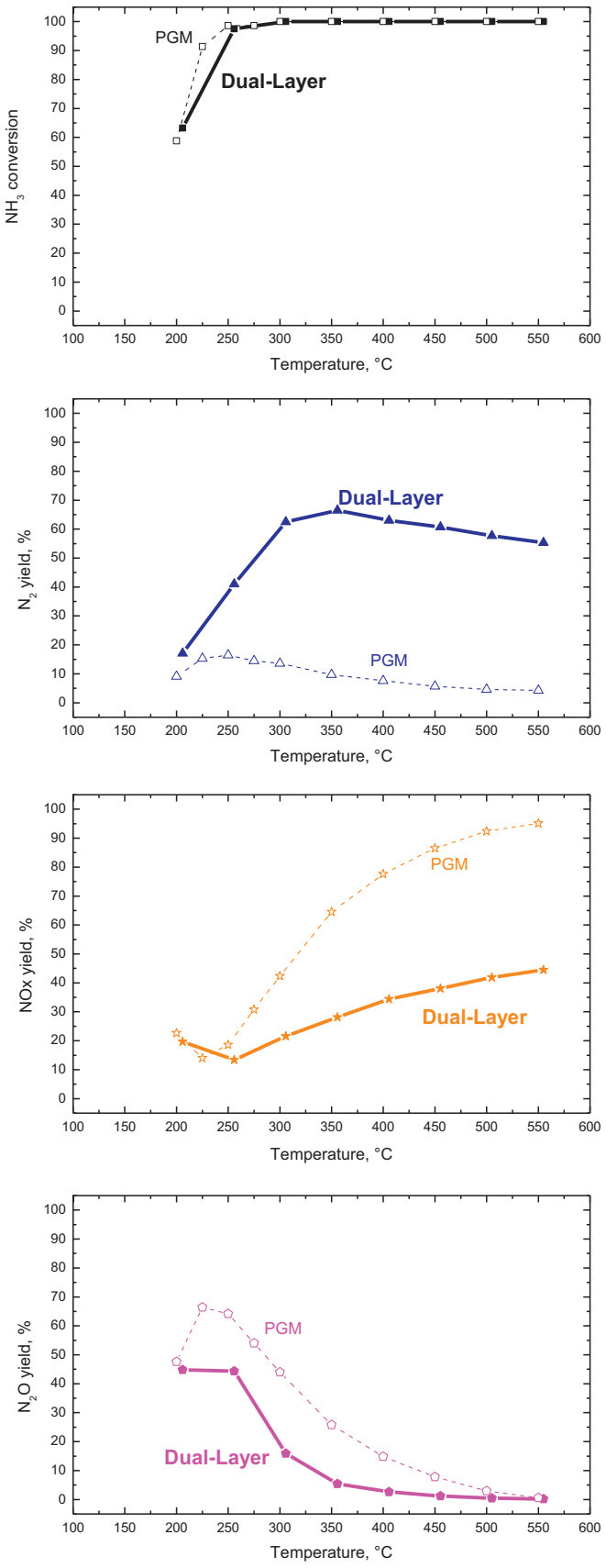

Fig. 4. NH_3/NO_x reacting system on ASC dual-layer monolith (thick lines) vs. PGM monolith (dashed lines). NH_3 = 500 ppm; NO_x = 500 ppm; NO_2/NO_x = 0; H_2O = 8% (v/v); O_2 = 8% (v/v); CO_2 = 8% (v/v), GHSV = 100,000 h^{-1} (N_2 amount calculated from N-balance).

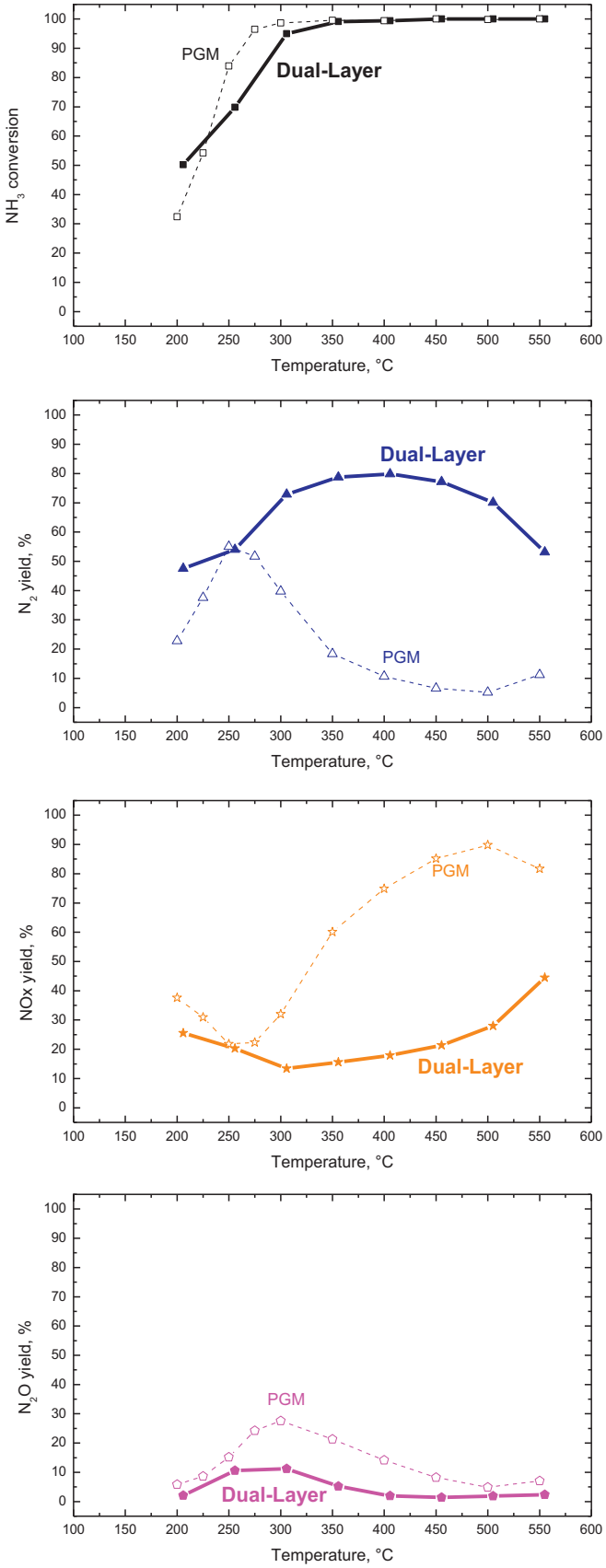

Fig. 5. NH_3/NO_x reacting system on ASC dual-layer monolith (thick lines) vs. PGM monolith (dashed lines). NH_3 = 500 ppm; NO_x = 500 ppm; NO_2/NO_x = 1.0; H_2O = 8% (v/v); O_2 = 8% (v/v); CO_2 = 8% (v/v), GHSV = 100,000 h^{-1} (N_2 amount calculated from N-balance).

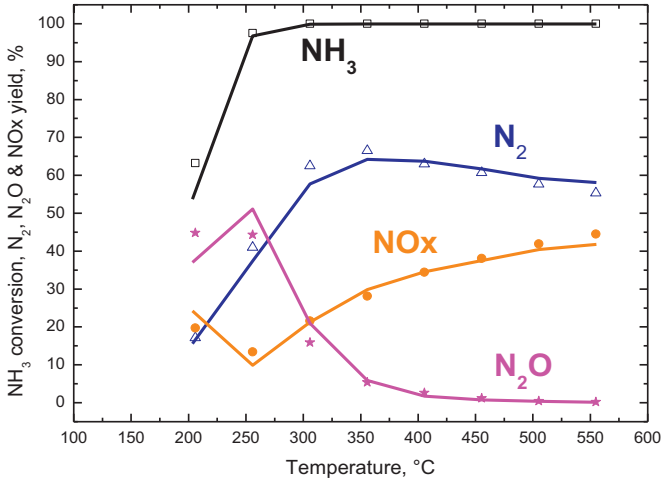

Fig. 6. NH_3/NO_x reacting system on ASC dual-layer monolith: NH_3 = 500 ppm; NO_x = 500 ppm; NO_2/NO_x = 0; H_2O = 8% (v/v); O_2 = 8% (v/v); CO_2 = 8% (v/v), GHSV = 100,000 h^{-1} (N_2 amount calculated from N-balance). Symbols: experimental results; lines: model simulations.

N_2 selectivity, with a corresponding decrease in the formation of undesired products, namely NO_x and N_2O. Notably, no significant effects of diffusional limitations related to the SCR layer were observed, at least in the investigated range of operative conditions. In particular, no significant reduction of NH_3 conversion was detected. On the opposite, the presence of the SCR layer enhanced the NH_3 conversion thanks to the occurrence of the N_2 selective NH_3-SCR reactions. This effect was found to be more pronounced when NO_2 was present at reactor inlet, in line with the high sensitivity of the NH_3-SCR rates to the NO_2/NO_x feed ratio observed over the Fe-zeolite SCR component in [6].

3.3. Validation of the dual-layer ASC simulation model

After independently validating the SCR [6] and the PGM kinetics (Section 3.1), the same rate expressions and rate parameters were incorporated into the full dual-layer NH_3 slip monolith model developed in [8]. Additionally, all the relevant geometrical and morphological properties of the monolith sample were also integrated in the same model, which was then validated against experimental data collected over the dual-layer core monolith sample.

Figs. 6 and 7 show a direct comparison between experimental data (dots) and model simulations (solid lines) for the different reacting systems (500 ppm of NH_3 and NO_x (NO_2/NO_x = 0 and 1) with 8% (v/v) of H_2O, O_2 and CO_2 in N_2). Additional validation results for the cases of NO_2/NO_x = 0.25, 0.5 and 0.75 are provided as supplementary material (Figures G to I). The simulation results were obtained after a modest adjustment of the PGM rate parameters accounting for NO_2 inhibition in the denominators of the two rate equations for NH_3 and NO oxidation. The need for such an adjustment may originate from: (i) the empirical kinetic description of the observed NO_2 inhibition effect, based on a simple LHHW-type term depending on the gas phase NO_2 concentration [7]; (ii) the uncertainty affecting the local NO_2 concentrations at the SCR/PGM interface of the ASC, being determined by diffusion/reaction in the SCR catalyst layer. In any case the changes in the rate parameters affect the simulation results only at conditions where excess NO_2 is present, which is not the most common situation over an ammonia slip catalyst.

As evident from the Figures, a generally good agreement was observed in terms of both NH_3 conversion and products yields, with the most evident deviations recorded in the case of NO_2/NO_x

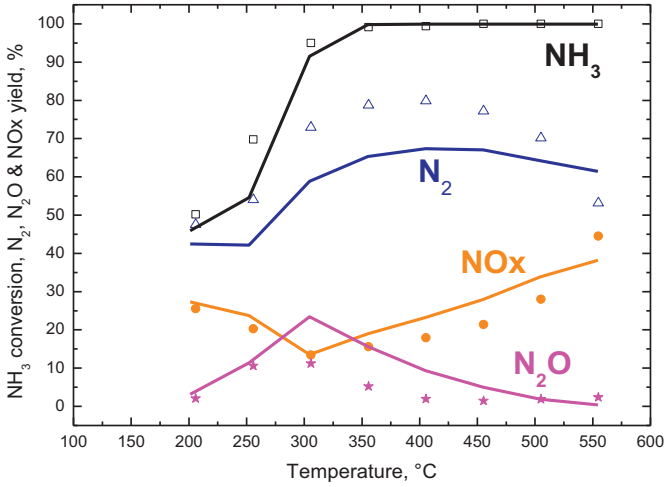

Fig. 7. NH_3/NO_x reacting system on ASC dual-layer monolith: NH_3 = 500 ppm; NO_x = 500 ppm; NO_2/NO_x = 1; H_2O = 8% (v/v); O_2 = 8% (v/v); CO_2 = 8% (v/v), GHSV = 100,000 h^{-1} (N_2 amount calculated from N-balance). Symbols: experimental results; lines: model simulations.

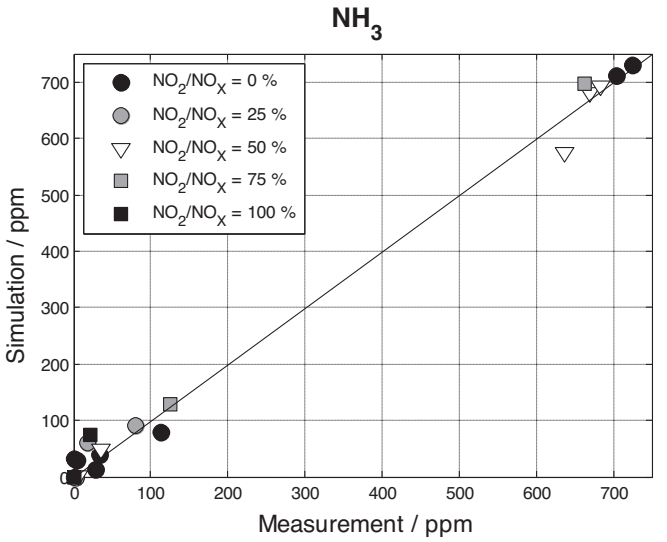

Fig. 8. DOE experiments on ASC dual-layer monolith: NH_3 measured vs. simulated concentrations.

feed ratios of 0.5 and 1. In the first case (Figure H in supplementary material), minor differences between experimental data and simulations were evident at temperatures as high as 300 °C, while further increasing the catalyst temperature resulted in the underestimation of the N_2 yield and a corresponding overestimation of the NO_x one. In the case of NO_2/NO_x = 1 (Fig. 7), the model predicted again a lower N_2 yield in comparison with what experimentally observed, with a corresponding overestimation of the NO_x and N_2O yields.

Further validation of the ASC model has been carried out with steady state measurement data from a gas test bench which cover the full range of operation relevant for the ASC (see ranges in Table 1). Indeed, the first set of model validation runs included only a limited number of operating conditions for the ASC, and all the experimental tests were carried out at GHSV = 100,000 h^{-1}, which represents a low space velocity for an ammonia slip catalyst under real operating conditions. The range of tested space velocities is extended here up to GHSV = 300,000 h^{-1}.

The operation points considered here consist of two groups. The first group was chosen according to a DoE plan to ensure the correct parameterization of an empirical DoE-model, which has been developed in parallel to the present physically/chemically based ASC model. To set up the DoE plan the AVL tool Cameo was used. The selected model was cubic with second order interactions. Physically illogical operation areas (e.g. 100% NO_2/NO_x feed ratio at $T > 350$ °C) were excluded from the model setup at the beginning. The DoE software chose 21 operation points whereof 7 are repetition points (SV = 150,000 h^{-1}, at NH_3/NO_x (alpha) = 2, NO_2/NO_x = 50%, T = 300 °C). Further, a second group of 30 additional operation points was chosen in order to obtain a systematic pattern over the whole operation range, according to the approach usually followed in the development process of after treatment systems. The additional data included another repetition point at a space velocity of 30,000 h^{-1}, again at NH_3/NO_x(alpha) = 2, NO_2/NO_x = 50% and 300 °C. The chosen operation points are displayed in Figure J in supplementary material where the blue rhombs represent the points chosen by the DoE tool and the red dots those chosen in addition.

The confidence interval of the received measurement data was set to 95%. While higher confidence intervals occurred for the outlet concentrations, N_2O shows the largest confidence interval (±5 ppm). The deviation for the repetition point at SV = 30,000 h^{-1} for the inlet and outlet concentration of the measurement is displayed in Figure K in supplementary material.

Despite the fact that more repetition points were taken for a space velocity of 150,000 h^{-1}, it is still found (Figure L in supplementary material) that the confidence interval for the outlet concentration is higher for all measured species if compared to a space velocity of 30,000 h^{-1}. This is most likely due to the fact that higher space velocities lead to higher uncertainties in the measured concentrations.

Figs. 8–10 illustrate the comparison of measured vs. simulated data throughout the full DoE range for NH_3, NO and N_2O. NO_2 content is always below 75 ppm, its comparison is shown in Figure M in supplementary material. N_2 is calculated from the

Table 1
Range of operating conditions investigated in the ASC catalyst study.

Space velocity [h^{-1}]	Temperature [°C]	NH_3/NO_x	NO_2/NO_x
30,000–300,000	180–500	0–20	0–1

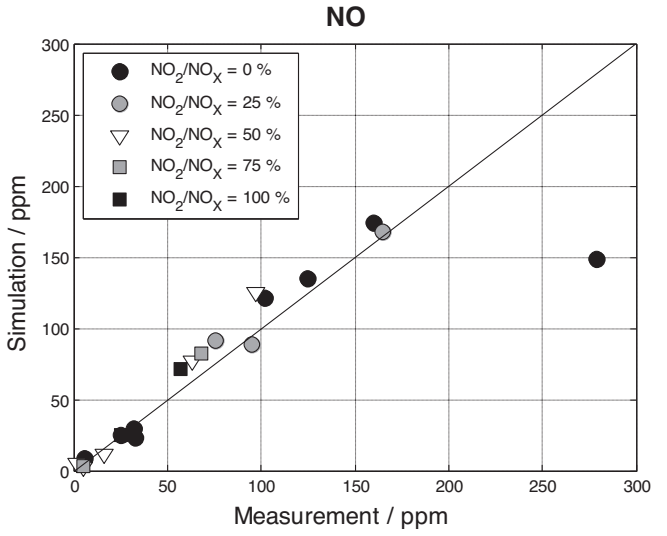

Fig. 9. DOE experiments on ASC dual-layer monolith: NO measured vs. simulated concentrations.

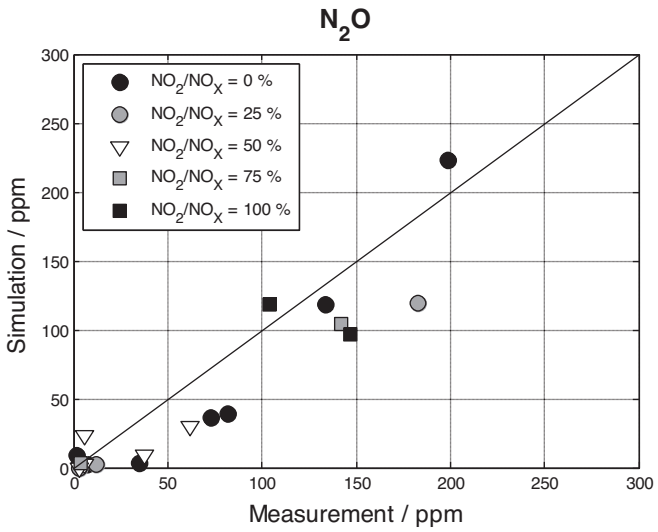

Fig. 10. DOE experiments on ASC dual-layer monolith: N_2O measured vs. simulated concentrations.

N-balance and therefore not displayed. NH_3 exhibits the best agreement between simulation and measurements (Fig. 8). Despite the generally good agreement for NO and NO_2 (Fig. 9 and M) in simulation vs. measurement, one can still find one data point with high deviation. This data point corresponds to a space velocity of 150,000 h^{-1}, a temperature of 450 °C and a NO_2/NO_x ratio of 0%. Taking the comparison of simulated data vs. measured data into account (e.g. SV = 275,000 h^{-1}, T = 350 °C, NO_2/NO_x = 0% or SV = 150,000 h^{-1}, T = 500 °C, NO_2/NO_x = 0%) this particular data point seems hardly in line with the other data measured under similar operation conditions. Hence the measurement of this operation point is considered as an outlier.

The highest deviation between measurement and simulation over the full data range is observed for N_2O, cf. Fig. 10. However, a systematic trend of over- or underestimation of N_2O by the model cannot be detected. This result is in line with the highest confidence interval of the measured N_2O data. The simulation of the end of pipe NO_2 content can play an important role as NO_2 emissions might be limited in future. The model slightly under estimates the NO_2/NO_x ratio after ASC for most of the DoE points, cf. the comparison to the measured values shown in Figure N in supplementary material. This could be eventually improved by enhancing the NO oxidation activity of either the PGM or the SCR layer.

4. Conclusions

The work herein reported concludes the development of a chemically and physically consistent mathematical model of commercial dual-layer (SCR + PGM) monolithic NH_3 slip converters (ASC).

In this Part 2 of the project we have first validated the global kinetic model for the PGM component, previously developed over the precursor catalyst powders, against data collected over a single-layer coated monolith. Then, we have incorporated validated kinetics for the two individual SCR and PGM components into a dual-layer ASC monolith catalyst model and compared its predictions against extensive experimental catalytic activity data collected over core samples of the dual-layer ASC system. A DOE approach has been adopted to design the experimental plan in order to secure a uniform coverage of the operating field over a wide range of representative conditions. Results prove that the dual-layer ASC model can simulate realistically the performances of the actual NH_3 slip catalyst configuration, essentially on a predictive basis.

From a fundamental perspective, the present results emphasize the beneficial features of a dual-layer ASC configuration with the SCR catalyst on top of the PGM component. In Part 1 of this work, comparative experiments over a double bed and over a mechanical mixture of SCR and PGM catalyst powders had clearly pointed out a positive interaction between the PGM and the SCR catalytic chemistries. The N_2 selectivity was found significantly greater in the $NH_3 + O_2$ or $NH_3 + NO_x + O_2$ runs over the mechanical mixture configuration due to the possibility for the unselective NH_3 oxidation products (NO_x) formed over the PGM catalyst to further react selectively with NH_3 to N_2 over the SCR catalyst. In the present Part 2 such a positive interaction is confirmed and emphasized by the data collected over the dual-layer SCR + PGM monolith catalyst. We have shown in fact that the dual-layer architecture grants largely enhanced N_2 selectivities compared to a single-layer PGM-only washcoat: as the unselective NH_3 oxidation products (NO_x) formed over the PGM catalyst counter diffuse across the SCR catalyst layer, they have a chance to be reduced selectively to N_2 by the residual NH_3. Thus, the investigated configuration combines synergistically the high NH_3 conversion activity of the PGM layer with the NO_x reduction functionality and high N_2 selectivity of the SCR layer. Such important interactions between the PGM and SCR chemistries, coupled through diffusion/reaction in the SCR layer, are nicely captured by the developed ASC model.

From an applied perspective, thus, our work clearly demonstrates that, with such a dual-layer ASC brick placed behind an NH_3-SCR converter, minimal NH_3 breakthrough at increased NO_x conversion is possible. Modeling of ASC catalysts not only helps in rationalizing such synergistic effects, but is indeed necessary for an efficient development process of modern exhaust after treatment systems of high complexity and for the optimization of their operating strategies.

Appendix A. Supplementary data

Supplementary data associated with this article can be found, in the online version, at http://dx.doi.org/10.1016/j.apcatb.2013.05.032.

References

[1] A. Scheuer, W. Hauptmann, A. Drochner, J. Gieshoff, H. Vogel, M. Votsmeier, Applied Catalysis B: Environmental (2011).
[2] A. Scheuer, M. Votsmeier, J. Gieshoff, A. Drochner, H. Vogel, 6th International Conference on Environmental Catalysis, Beijing, China, 2010.
[3] A. Scheuer, W. Hauptmann, A. Drochner, J. Gieshoff, H. Vogel, M. Votsmeier, Applied Catalysis B: Environmental 111–112 (2012) 445–455.
[4] A. Scheuer, M. Votsmeier, A. Schuler, J. Gieshoff, A. Drochner, H. Vogel, Topics in Catalysis 52 (2009) 1847–1851.
[5] S. Shrestha, M. Harold, K. Kamasamudram, A. Yezerets, Topics in Catalysis (2013) 1–5.
[6] M. Colombo, I. Nova, E. Tronconi, V. Schmeißer, B. Bandl-Konrad, L. Zimmermann, Applied Catalysis B: Environmental 111–112 (2011) 106–118.
[7] M. Colombo, I. Nova, E. Tronconi, V. Schmeißer, B. Bandl-Konrad, Applied Catalysis B: Environmental (2013), http://dx.doi.org/10.1016/j.apcatb.2012.10.031.
[8] M. Colombo, I. Nova, E. Tronconi, Chemical Engineering Science 75 (2012) 75–83.
[9] D. Chatterjee, T. Burkhardt, B. Bandl-Konrad, T. Braun, E. Tronconi, I. Nova, C. Ciardelli, SAE Technical Paper 2005-01-0965, 2005.
[10] D. Chatterjee, T. Burkhardt, M. Weibel, I. Nova, A. Grossale, E. Tronconi, SAE Technical Paper 2007-01-1136, 2007.
[11] D. Chatterjee, T. Burkhardt, M. Weibel, E. Tronconi, I. Nova, C. Ciardelli, SAE Technical Paper 2006-01-0468, 2006.